ADVANCED ENERGY MATERIALS

Supporting Information

for *Adv. Energy Mater.,* DOI: 10.1002/aenm.201803260

Defect-Rich Soft Carbon Porous Nanosheets for Fast and High-Capacity Sodium-Ion Storage

Xuhui Yao, Yajie Ke, Wenhao Ren, Xuanpeng Wang, Fangyu Xiong, Wei Yang, Mingsheng Qin, Qi Li, and Liqiang Mai**

Supporting Information

Defect-Rich Soft Carbon Porous Nanosheets for Fast and High-Capacity Sodium-Ion Storage

Xuhui Yao, Yajie Ke, Wenhao Ren, Xuanpeng Wang, Fangyu Xiong, Wei Yang, Mingsheng Qin, Qi Li* and Liqiang Mai*

Calculation of Na^+ diffusion coefficients through GITT results: The D^{GITT} can be obtained from the potential response to a small constant current pulse via the following equation:

$$D^{GITT} = \frac{4}{\pi\tau}(\frac{m_B V_M}{M_B S})^2(\frac{\Delta E_S}{\Delta E_\tau})^2$$

Where τ is the constant current pulse time, S is the electrode–electrolyte interface area, m_B, M_B and V_M are the mass, molar mass and molar volume of SC-NS, respectively. ΔE_S is the voltage difference during the open circuit period, and ΔE_τ is the total change of cell voltage during a constant current pulse excluding the IR drop (Figure S13).

Calculation of Na^+ apparent diffusion coefficients through EIS results: The diffusion coefficient value (D^{EIS}) can be calculated from the following equation:

$$Z' = R_\varepsilon + R_{ct} + \sigma_w \omega^{-\frac{1}{2}}$$

$$D = 0.5(\frac{RT}{An^2F^2\sigma_w C})^2$$

Where $\omega(2\pi f)$ is the angular frequency in the low frequency region, and both R_e and R_{ct} are kinetics parameters independent of frequency. Then, the Warburg coefficient (σ_w) can be obtained from the slope of the fitting line. R is the gas constant, T is the temperature, A is the

area of the electrode, n is the number of electron transfer per mole of the active material involved in the electrode reaction, F is Faraday's constant and C is the molar concentration of Na ions.

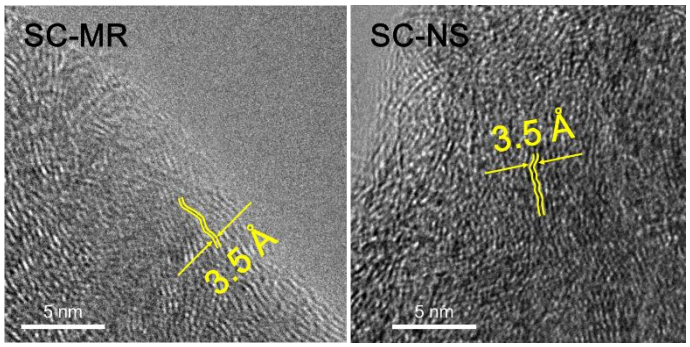

Figure S1. The high-resolution transmission electron microscopy image of SC-MR and SC-NS.

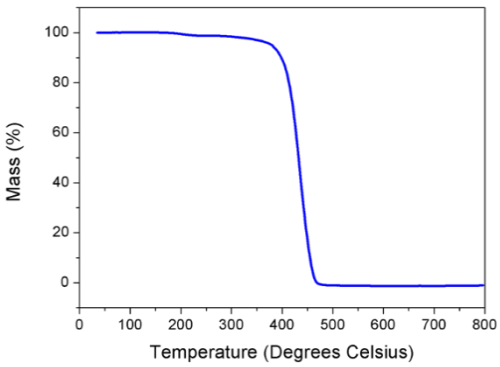

Figure S2. Thermogravimetry curve of polyvinylpyrrolidone obtained at argon atmosphere from room temperature to 800 °C.

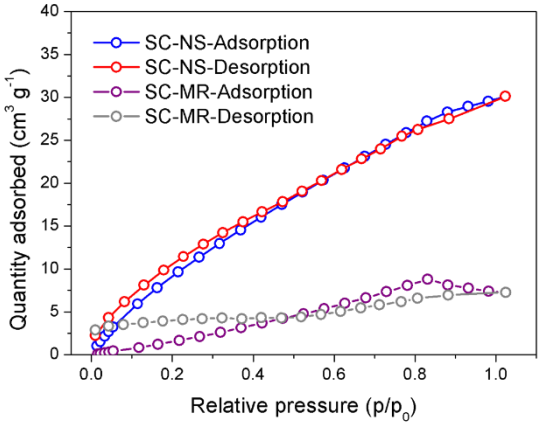

Figure S3. The CO_2 adsorption-desorption isotherms at 273 K.

Table S4. Raman bands and vibration modes for graphite

Band	Raman shift	Symmetry	Vibration mode
G	~1580 cm^{-1}	E_{2g}	Ideal graphitic lattice
D1	~1350 cm^{-1}	A_{1g}	Graphene layer edges
D2	~1620 cm^{-1}	E_{2g}	Surface graphene layer
D3	~1490 cm^{-1}	Line shape	Amorphous carbon
D4	~1200 cm^{-1}	A_{1g}	Polyenes, ionic impurities

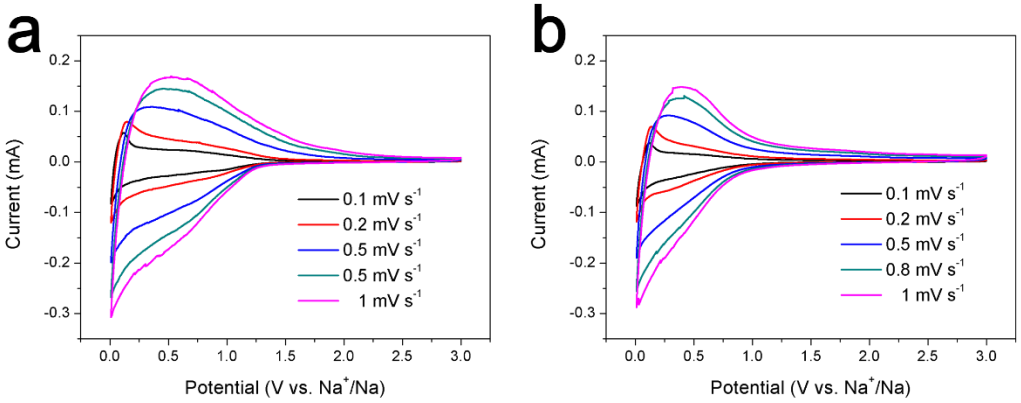

Figure S5. The CV results of (a) SC-NS and (b) SC-MR under an increasing voltammetric scan rates (from 0.1 to 1 mV s^{-1}).

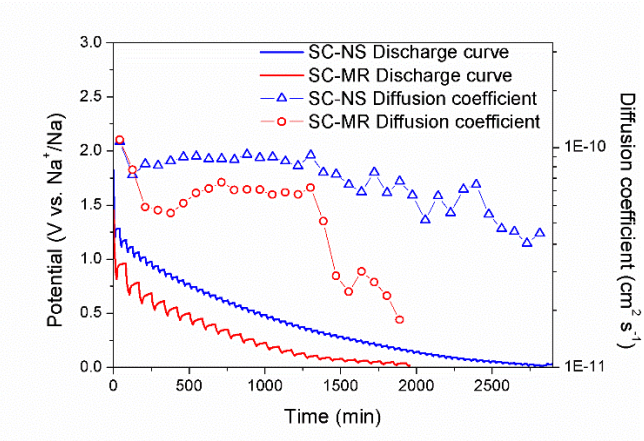

Figure S6. The discharge curves and calculated diffusion coefficients of two samples versus time of discharge.

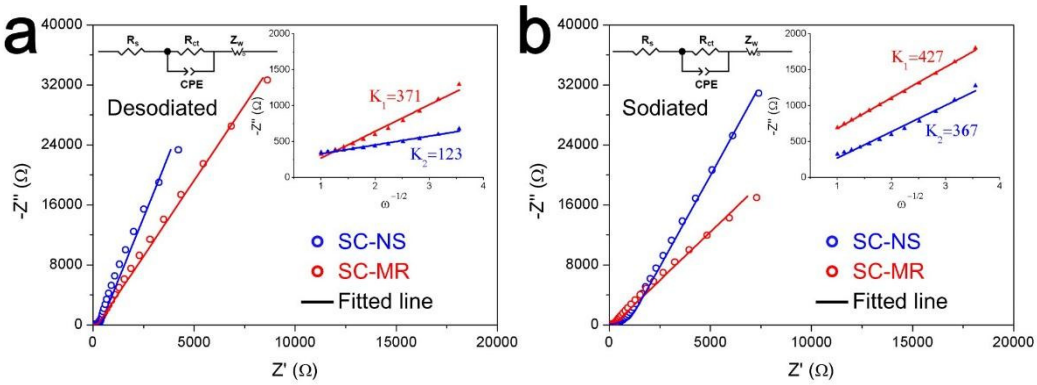

Figure S7. EIS results of (a) desodiated and (b) sodiated state of SC-NS (blue) and SC-MR (red), inset is the calculation of Warburg factor. In the desodiated state, the D^{EIS} calculated from the Warburg factor is 3.65×10^{-10} cm^2 s^{-1} and 4.03×10^{-11} cm^2 s^{-1} for SC-NS and SC-MR, respectively. After the sodiation, the D^{EIS} of SC-NS and SC-MR decrease to 4.06×10^{-11} and 3.04×10^{-11} cm^2 s^{-1}, which is consistent with the GITT results.

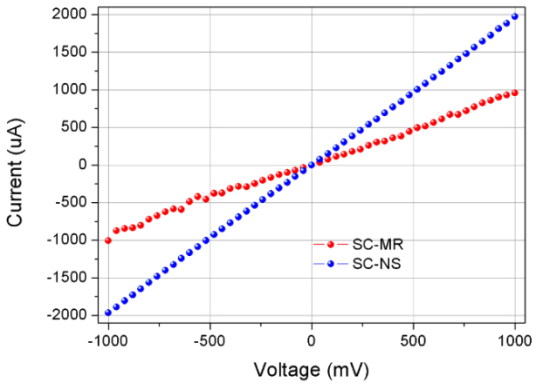

Figure S8. The I-V transport measurements of two samples.

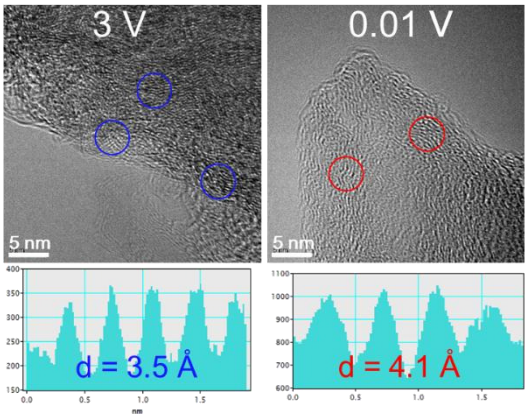

Figure S9. HR-TEM images and lattice fringes of SC-NS electrode at the different states.

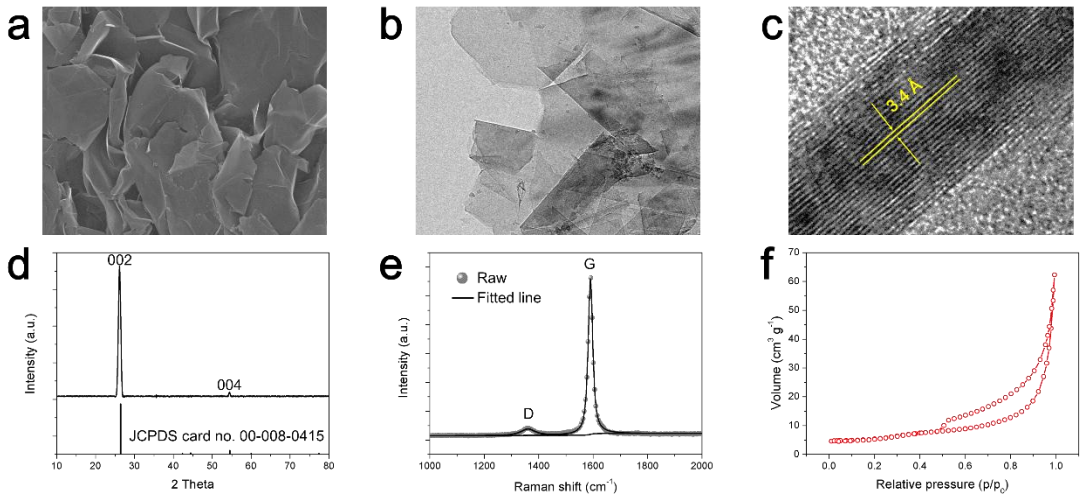

Figure S10. The morphology, structure characterization of expanded graphite (EG):

(a) FE-SEM and (b) TEM images of EG display a network of interconnected sheet-like morphology. (c) HR-TEM images of EG shows the lattice fringes of 3.4 Å, demonstrating a

typical graphitic structure. (d) XRD peaks are fully indexed to the graphite peaks (JCPDS card no. 00-008-0415). (e) Raman spectrum suggest that the EG has ideal graphitic lattice (G-band) with bits of disorder (D-band). (f) EG sample shows a type-III nitrogen adsorption-desorption isotherms with H3 hysteresis loop, suggesting plate-like structure and the BET surface area is 94.8 m^2 g^{-1}.

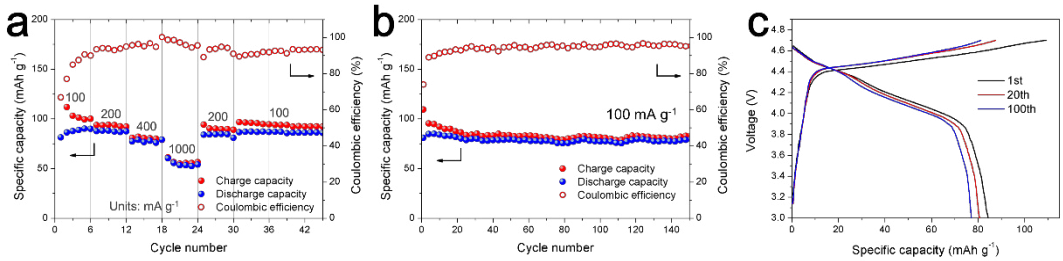

Figure S11. The electrochemical performance of EG: (a) The rate performance shows the capabilities of 103.1, 93.5, 80.5 and 55.6 mAh g^{-1} at current density of 100, 200, 400 and 1000 mA g^{-1}. (b) Cycling performance shows the first charge and discharge capacities of 121.6 and 81.4 mAh g^{-1}, respectively. A reversible capacity over 80 mAh g^{-1} could be maintained in the following 140 cycles. (c) The typical voltage profile shows that the major capacity contribution comes from the voltage plateau over 4.0 V.

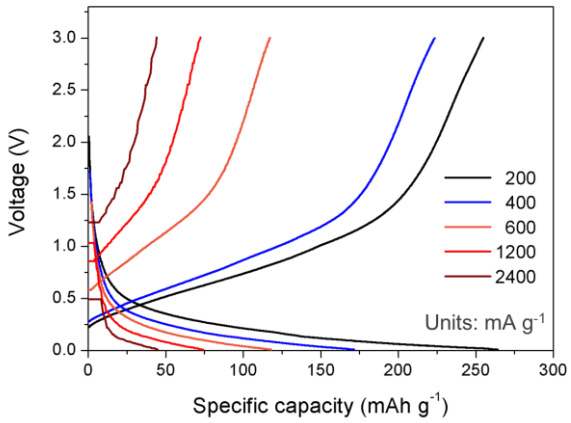

Figure S12. The charge-discharge curves of SC-MR electrode as potassium-ion battery anode at different current densities.

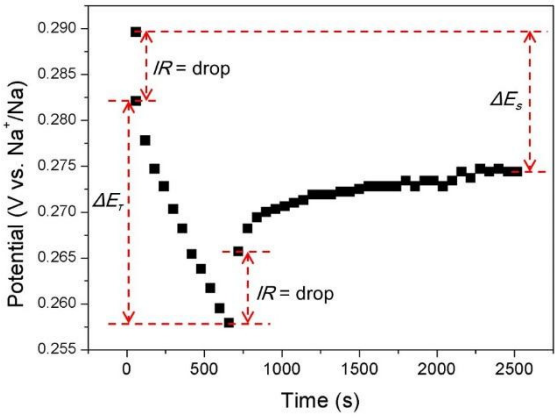

Figure S13. Galvanostatic intermittent titration technique (GITT) potential response curve with time.